NUMERICAL STUDY ON FLOW AND HEAT TRANSFER CHARACTERISTICS IN STRUCTURED PACKED BED

Nan LI [a*], Peng FENG [b], Jie CUI [a], Fan LI [a]，Jiawei SONG [a]

[a]School of Energy and Power Engineering, Shenyang Institute of Engineering, Shenyang, China

[b]Liao Ning Municipal Engineering Design&Research Institute Co., Ltd., Shenyang, China

* Corresponding author; E-mail: linanneu@163.com

ANSYS software is introduced to reproduce the in-line and staggered sphere packed bed model. To investigate the influence of model on the heat transfer and flow characteristics in the high temperature packed bed, numerical simulations of pore-level was used to numerically appreciate the changes of pressure drop, temperature and velocity. The simulation values qualitatively agree with the experimental result. The results show that the pressure drop in high temperature packed bed increases significantly. The pressure drop increases about 3200 Pa when the inlet velocity is 0.33-0.73 m/s. The model has significant influence on the average temperature of solid and gas phases. Compared with the in-line arrangement, the heat wave transfer is slower and the temperature is slightly higher by 20 K in the staggered model. The average velocity in the structured packed bed increases and decreases periodically. In staggered model, the velocity disturbance is more significant. These findings are helpful for understanding transport phenomena in packed beds as well as the design of high efficiency reactors.

Key words*: spherical porous media, packed structure, temperature distribution, flow*

1. Introduction

Porous media packed bed is widely used in engineering applications such as pebble bed combustion furnace, high temperature gas-cooled nuclear reactors and thermal energy storage and so on. Many scholars have carried out a lot of experimental and numerical research on it [1-6]. In numerical study, earlier research was based on macroscopic description [7, 8], that is, the complex porous system was regarded as a uniformly distributed virtual continuous medium, which simplifies the complex internal flow and heat transfer, but this method concealed the essential characteristics of the flow in pores. With the continuous improvement of computer performance, mesoscopic methods based on pore scale have come into being. In this method, the detailed porous media structure is established to reveal the heat transport process in the pore scale and study the effect of pore structure on flow heat transfer.

Calis *et al.* [9] and Romkes *et al.* [10] investigated numerical simulation and experimental research on the mass and heat transfer characteristics of a composite structured packing (CSP). The CSP consisted of a number of square tubes filled with spherical particles, in which the particles formed five kinds of orderly arrangements. The convective heat transfer results obtained by numerical

simulation were in good agreement with the experimental results. The results show that there are some differences in the convective heat transfer characteristics of fluid in porous media with different particle packing modes. Gunjal *et al.* [11] numerically studied the convective heat transfer in cells of four kinds of porous media with orderly packed particles such as simple cubical, 1-D rhombohedral, 3-D rhombohedral, and face-centered cubical geometries, and found that the velocity distribution and path lines were completely different when the arrangement was different. Yang *et al.* [12] constructed 3D packed bed models of porous media pellets with spherical particles. The effects of Reynolds number and packing form on the performances of forced convection heat transfer in porous media are investigated in detail. The results show that, the overall heat transfer performance of uniform packing is much better than that of the non-uniform packing. Zhu *et al.* [13] studied the flow and heat transfer of solar receivers with three packed types, and the results showed that the packed type had a significant impact on pressure drop and comprehensive heat transfer efficiency. Kim *et al.* [14] have proved that the structured packing configurations, such as the simple cubic (SC) packing, the body-centered cubic (BCC) packing and the face-centered cubic (FCC) packing have different heat/mass transfer characteristics compared with the traditional randomly packed beds. Wang *et al.* [15] numerically studied characteristics of fluid flow, heat transfer and methane steam reforming reaction in packed beds with three different packing structures (SC, BCC and FCC) to explore the influence of dispersion on heat transfer and reaction performance.

The studies show that the particle stacking structure has a great influence on the flow and heat transfer performance in the packed bed. However, the current research mainly focuses on the flow field at normal temperature and low temperature, and the research on the high temperature packed bed is relatively lacking. Since the physical properties of the gas phase and the solid phase are significantly different, there are obvious non-equilibrium characteristics of flow and heat in the whole system when the temperature is high, so it is necessary to further study the flow and heat transfer characteristics in the system. Therefore, the purpose of this work is to explore the heat transfer and flow properties of the packed bed with different packing forms in high temperature flow field, and try to get the mechanism of affecting the heat transfer and flow in packed bed, and provide the detailed information for designing high-performance of structured packed beds.

2. Physical model

The porous packed bed under study was used by Zhdanok *et al.* [16] to study propagation of thermal wave. The thermally insulated burner was 76 mm in diameter with a length of 500 mm and composed randomly of 5.6 mm alumina spheres. The thermal characteristics of the bed by initially preheating a narrow zone and air flow the bed at 0.43 m/s was characterized. In this paper, in order to simplify the calculation, it is assumed that porous media pellets with a diameter of 5.6 mm were established in in-line and staggered packed model. The number of pellets and the geometric size of the calculation zone are shown in Tab.1. The total length of the computational domain is L, which is composed of the inlet zone $L1$, the porous zone $L2$ and the outlet zone $L3$. The lengths of $L1$ and $L3$ are 16.8 mm (3 times the distance of the diameter of the pellet) respectively, to avoid the influence of inlet and outlet effects on the flow heat transfer in the porous medium area. $L2$ length is reduced to about 260 mm, as it is able to reach the fully-developed state and meet the study purpose. In in-line packed model, the center distance between the contacting spheres is equal. There are 46 spheres along the gas flow direction, and the length of $L2$ is 257.6 mm. The total calculated length L is 291.2 mm,

and the porosity is 0.476. In staggered packed model, the center distance between the contacting spheres is an isosceles triangle, and there are 53 spheres arranged. The length of $L2$ is 257.8 mm, the total length of L is 291.4 mm, and the porosity is 0.4. Due to the limitation of calculation conditions, it is difficult to simulate the flow heat transfer in 3D packed beds by using the pore scale method, and the spheres arrangement channels are symmetrical along the x and y axes. Therefore, along the airflow direction, 1/4 sphere channel is selected as the calculation zone, namely -1.4 mm≤x≤1.4 mm, -1.4 mm≤y≤1.4 mm, 0≤z≤L, as shown in Fig.1 and 2. In this study, alumina was used as porous medium pellet, and their physical parameters are: density 2500 kgm^{-3}, specific heat capacity at constant pressure 1300 $Jkg^{-1}K^{-1}$, absorption coefficient 104.9 m^{-1} and thermal conductivity 2.02 $Wm^{-1}K^{-1}$ [17]..

Table 1. Physical model geometry

structure	L1(mm)	L2(mm)	L3(mm)	L(mm)	Number of 1/4 pellets
in-line	16.8	257.6	16.8	291.2	46
staggered	16.8	257.8	16.8	291.4	53

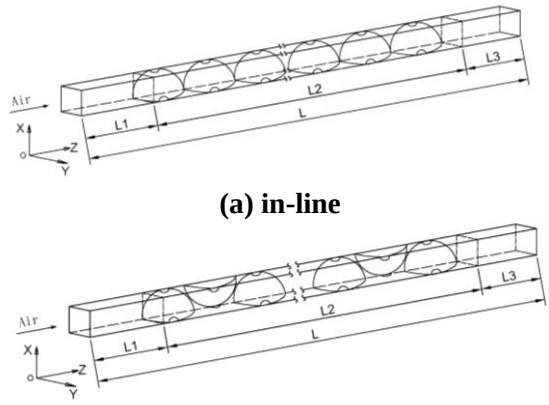

(a) in-line

(b) staggered

Figure 1. 3D diagram of packed bed

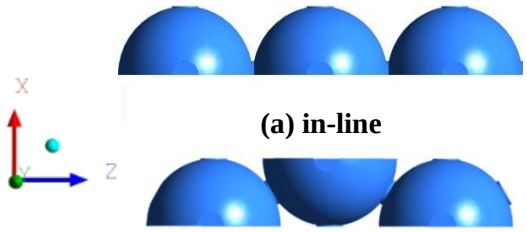

(a) in-line

(b) staggered

Figure 2. Pellets channel

2.1. Numerical simulation method

The following assumptions are made to simplify the problem:

- The inlet velocity of air is low and the Reynolds number is rather small. The gas flow is assumed to be laminar**.**
- The gas is an incompressible ideal fluid and the gas radiation is ignored.
- The alumina pellets are non-transparent materials, and the scattering of the sphere surface is ignored. The radiative heat transfer between the spheres surfaces uses the Discrete Coordinate Radiation (DO) model.
- The wall of the packed bed is a symmetrical surface.

Governing equations

(1) Continuity Equation：

$$\frac{\partial(\rho_g)}{\partial t} + \nabla \bullet (\rho_g \vec{v}) = 0 \tag{1}$$

（2）Momentum Equation：

$$\frac{\partial(\rho_g \vec{v})}{\partial t} + \nabla \bullet (\rho_g \vec{v}\vec{v}) = -\nabla P + \nabla \bullet (\mu \nabla \vec{v}) \tag{2}$$

(3) Solid energy equation：

$$\frac{\partial(\rho_s c_s T_s)}{\partial t} + \nabla \bullet (\lambda_s \nabla T_s) = 0 \tag{3}$$

（4）Gas energy equation：

$$\frac{\partial(\rho_g c_g T_g)}{\partial t} + \nabla \bullet (\rho_g c_g u_g \nabla T_g) = \nabla \bullet (\lambda_g \nabla T_g) + q_R \tag{4}$$

Where ρ_g, u_g, c_g, λ_g and T_g are gas density, velocity, specific heat capacity, thermal conductivity, temperature respectively. $\vec{\mathbf{v}}$ is velocity vector, t is time, P is pressure, μ is dynamic viscosity, ρ_s, c_s ,λ_s and T_s are porous media density, specific heat capacity, thermal conductivity, temperature, respectively. q_R is radiant heat flux.

2.2. Boundary conditions

The walls are symmetrical, and the boundary conditions are as follows:

$$\left\{\begin{array}{ll} z = 0 & T = T_0, u_z = u_0, u_x = u_y = 0 \\ z = L & \frac{\partial T}{\partial z} = \frac{\partial u_x}{\partial z} = \frac{\partial u_y}{\partial z} = \frac{\partial u_z}{\partial z} = 0 \\ x = \pm 1.4 & \frac{\partial T}{\partial x} = \frac{\partial u_y}{\partial x} = \frac{\partial u_z}{\partial x} = 0, u_x = 0 \\ y = \pm 1.4 & \frac{\partial T}{\partial y} = \frac{\partial u_x}{\partial y} = \frac{\partial u_z}{\partial y} = 0, u_y = 0 \\ pellet\ \ wall\ \ surface & u_x = u_y = u_z = 0 \end{array}\right\} \tag{5}$$

Where T_0 and u_0 are gas inlet temperature and gas inlet velocity respectively. L is the total length of the calculated zone, d is diameter of sphere.

Radiant heat loss from the inlet and outlet of the packed bed is computed as:

$$\lambda_s \frac{\partial T_s}{\partial z} = -\varepsilon_r \sigma (T^4_{s,in} - T^4_o) \tag{6}$$

$$\lambda_s \frac{\partial T_s}{\partial z} = -\varepsilon_r \sigma (T^4_{s,out} - T^4_o) \tag{7}$$

Where ε_r is the emissivity of pellet surface and set to be 0.4 [18], σ is Steffan-Boltzmann constant, $T_{s,in}$, $T_{s,\,out}$ is the temperature at inlet and outlet of pellet.

2.3. Initial conditions and solution method

As the working medium, air with an initial temperature of 300 K flows into the packed bed at 0.43 m/s, and the physical property parameters are constant, ρ= 1.205 kgm^{-3}, μ=1.8189×10^{-5} Nsm^{-2}. In the hot state, the physical properties of air such as thermal conductivity and viscosity are functions of

temperature and are calculated using kinetic theory. The initial temperature of pellets is set by UDF and is consistent with the initial preheating temperature of the packed bed at *t*=0s in Zhdanok *et al.* [16] experiment. The convergence criterion of gas and solid energy conservation equations is 10^{-6}, and other equations are 10^{-3}. The governing equation is a second-order upwind difference scheme, the fluid pressure-velocity coupling is solved based on SIMPLE method, and FLUENT16.0 is used for numerical calculation.

2.4. Grid and time step independence test

Meshing software was used to divide the mesh. In order to avoid the low-quality grids at the contact point of the adjacent pellets, "cylindrical bridge" was used to connect, assuming that the physical property of the "bridge" was the same as that of the pellet. According to Bu *et al.* [19], when the diameter of the cylinder is 16-20 % of the diameter of the sphere, the results will not be affected. Therefore, the model is established according to 20 % d in this paper. The contact between pellets is small, the grid is finer. Coarse mesh is used inside the pellet， as shown in Fig.3.

(a) in-line

(b) staggered

Figure 3. Computational grid

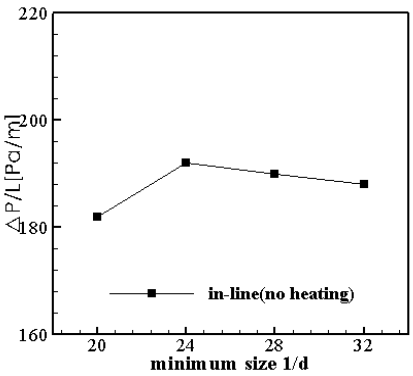

Figure 4. Variations of pressure drop with different meshes

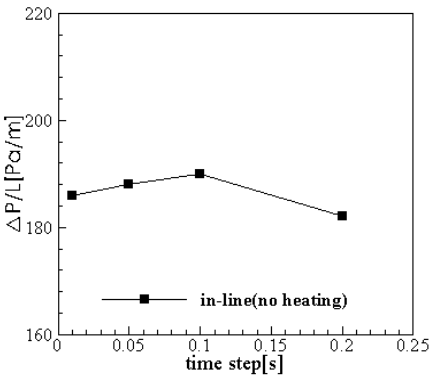

Figure 5. Variations of pressure drop with different time step

To ensure that the calculation results are reliable, a grid and time step independence test is taken. Firstly, the grid independence is tested, four sets of grids with the minimum size of the mesh elements sizes of d/20，d/24, d/28 and d/32 are tested. Fig. 4 presents the influence of mesh on the pressure drop in the in-line packed bed. When the minimum size of the mesh elements is d/28, the influence of mesh on the pressure drop is insignificant. The relative differences for pressure drop are less than 2 %.

Therefore, the d/28 is selected in the following study. It is finally obtained that the number of grids in the in-line and the staggered model is about 790,000 and 860,000, respectively.

Secondly, the independence of time step is tested. Fig.5 shows the variation of pressure drop in the in-line model when the time step is 0.01s, 0.05s, 0.1s and 0.5s respectively. On the basis of ensuring stability and saving computing resources, the time step is selected to be 0.1s. Therefore, the computational models used in this study are reliable and can be used in the following study.

3. Results and discussion

Figure 6 illustrates the experimental values of Zhdanok *et al.* [16] and the thermal wave predicted by the in-line and staggered models for an air inlet velocity of 0.43 m/s at 333s. In the experiment, the specific position of thermocouple in packed bed was not indicated, so the temperature at the alternating gas-solid phase (x=0 mm, y=0 mm, $0 \le z \le L$) was selected as the simulated temperature for analysis. As can be seen from the fig.4, both the simulated and experimental measurements have the same propagation trend, and they all change in the form of parabola. However, the simulated temperature is continuous but not smooth due to the thermal non-equilibrium. Compared with staggered arrangement, the temperature transfer of in-line arrangement is slightly faster. The simulated temperature is in good agreement with the experimental value in the low temperature area near the inlet and outlet. In the high temperature zone, the experimental value is slightly lower than the simulated temperature, and the relative error between them is about 6 %. This is mainly caused by the following reasons: firstly, the pellets are randomly arranged in the experiment, but they are simplified to orderly arrangement in the study, so there must be errors; secondly, the wall surface of the stacking bed model is symmetric and heat loss is not considered. But the error is within the allowable range, which verifies the effectiveness of the model and numerical method.

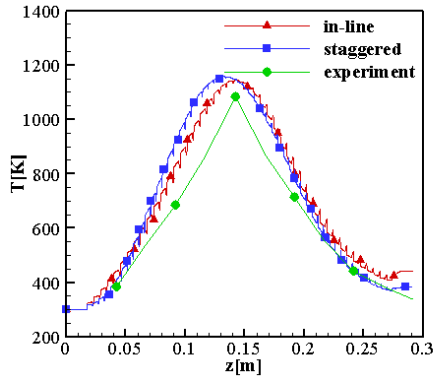

Figure 6. Temperature profiles of experiment and simulation（*t*=333s）

3.1. Pressure drop

Figure 7 displays the pressure drop of in-line and staggered models under no heating and heating conditions when u_0 is 0.33-0.73 m/s. As illustrated in Fig.7, the pressure drop increases obviously in the high temperature packed bed. In the steady cold flow field, the maximum pressure drop is 1520Pa, while in the hot flow field, the dynamic viscosity, flow resistance and pressure loss of air increase due to the temperature rise, and the maximum pressure loss is 4750 Pa. Compared with in-line model, the staggered model has greater pressure loss due to its lower porosity. With the increase of the velocity, the flow disturbance in the pore is intensified, the pressure loss increases

significantly, and the pressure drop increases faster in the staggered arrangement. Therefore, the choice of porosity shouldn't be too small to avoid the flow instability.

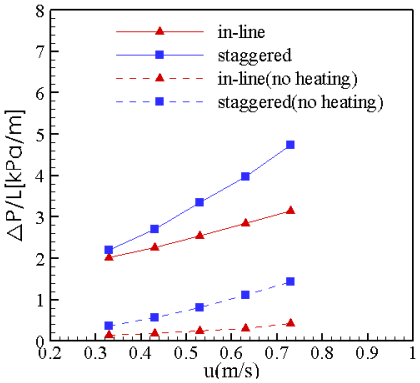

Figure 7. Pressure drop in the in-line and the staggered model

3.2. Temperature characteristic

The temperature characteristics in the structured packed bed are analyzed from three aspects: average temperature of packed bed ($\overline{T}$), solid phase average temperature ($\overline{T}_s$) and gas phase average temperature ($\overline{T}_g$). All of the simulation results used in this section for analysis are obtained with u_0=0.43 m/s at t=250 s.

Figure 8 shows $\overline{T}_s$ in in-line and staggered arrangement. As shown in the Fig.8, the temperature along the flow direction is parabolic. The temperature of in-line arrangement is not smooth, showing a "step" type, while the temperature of staggered arrangement is relatively smooth. The temperature of gas-solid phase in the packed bed is different, and the fluctuation of porosity along the flow direction leads to different degrees of temperature interference between gas and solid phase. As can be seen from Fig.2, the sparse in-line arrangement leads to large porosity fluctuation. When the air is close to the joint between spheres, the porosity increases gradually, and the influence of the gas phase on the $\overline{T}_s$ is enhanced. At the joint, the porosity reaches the maximum and the influence is the strongest. When the air far away from the joint, the influence is weakened, so the $\overline{T}_s$ fluctuates significantly, showing a "step" type. While the tight staggered distribution makes the porosity fluctuation relatively small, and $\overline{T}_s$ is less affected by the gas phase, so the temperature curve is relatively smooth.

Figure 9 shows the $\overline{T}_g$ in in-line and staggered arrangement. It is can be seen from that, the temperature of both are in a "zigzag" parabolic pattern. This shows that $\overline{T}_g$ fluctuates under the influence of the solid phase temperature along the flow direction. In the upstream and downstream regions of the highest temperature, the temperature oscillation is obvious, while in the high temperature region, the oscillation is gentle. This is due to the large temperature difference between the gas and the solid phase in the upstream and downstream regions. From the inlet of the packed bed, with the transfer of heat waves, heat conduction is carried out between the same phase through thermal conductivity and radiation, and heat exchange is carried out between the different phases through convective heat transfer. Therefore, the temperature difference between the gas and solid phases gradually decreases, and finally the thermal equilibrium is reached. In the downstream region, the temperature transfer between in-phase and two phases is also carried out by heat conduction and convective heat transfer. Affected by the arrangement model, the temperature oscillation amplitude is

slightly higher in the in-line model.

Meanwhile, compared with $\overline{T}_s$ in Fig.8, the temperature fluctuation range of the gas phase is relatively stronger, which is because the thermal diffusion rate of the solid phase is smaller than that of the gas phase, resulting in the temperature gradient change of the solid phase is smaller than that of the gas phase.

Figure 10 shows $\overline{T}$ with two models. The variation of form is between $\overline{T}_g$ and $\overline{T}_s$. Due to the existence of porous media, $\overline{T}$ fluctuates. When staggered, the heat wave transmission is slow, and the peak temperature is about 20 K higher than the in-line arrangement. At the upstream of the highest temperature, $\overline{T}$ of staggered is higher. At the downstream of the maximum temperature, $\overline{T}$ of ordered arrangement is slightly higher due to the heat wave transmission.

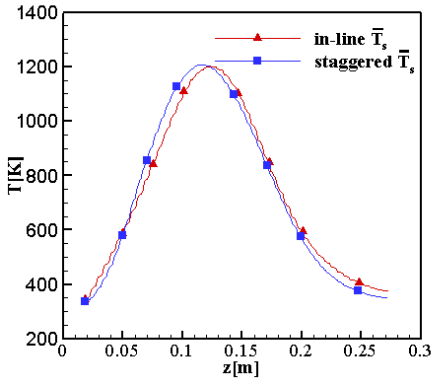

Figure 8. Average temperature of solid

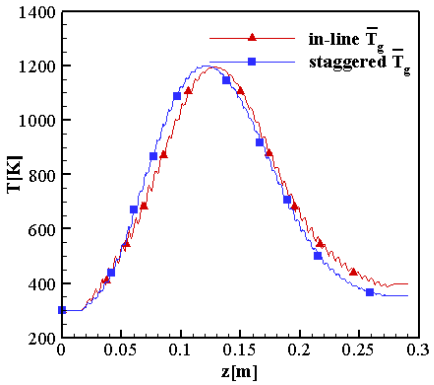

Figure 9. Average temperature of gas

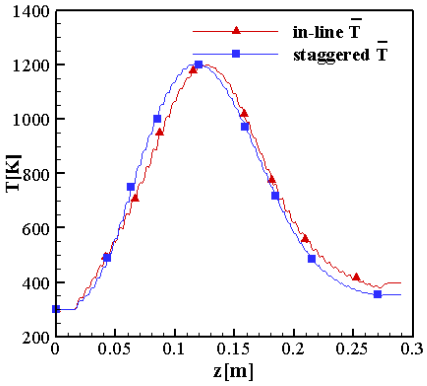

Figure 10. Average temperature of packed bed

3.3. Flow characteristic

The average velocity is obtained by integrating and averaging the velocities in different sections of the fluid region to illustrate the flow characteristics of the flow field. Fig.11 illustrates the distribution of the average velocity ($\bar{u}$) in the packed bed of in-line and staggered arranged pellets at u_0=0.43 m/s for t=250 s. It can be observed that, ū changes dramatically along the direction of the flow, indicating that the structure of the porous medium in the packed bed plays a key role in the velocity. In both in-line and staggered models, ū decreases when the airflow approaches the pellet between adjacent pellets. After the minimum value is reached, ū increases as the airflow moves away from the sphere, so that the velocity increases and decreases periodically inside the packed bed. Moreover, in the flow zone, the value of the maximum average velocity and the minimum average

velocity are similar to parabola due to the influence of the temperature field except for the inlet and outlet regions. $\bar{u}$ reaches the maximum when the temperature is the highest.

Due to the influence of model on the porosity, the peak value of $\bar{u}$ is 8.2 m/s in staggered model. In in-line model, the peak value of $\bar{u}$ is 7.8 m/s, and the speed difference between them is small. But the minimum average velocity changes slightly differently. In in-line, the velocity fluctuates gently, and the minimum velocity varies between 0.4-2.2 m/s. While the minimum velocity varies between 0.4-4 m/s in the staggered model. and the disturbance is intensified.

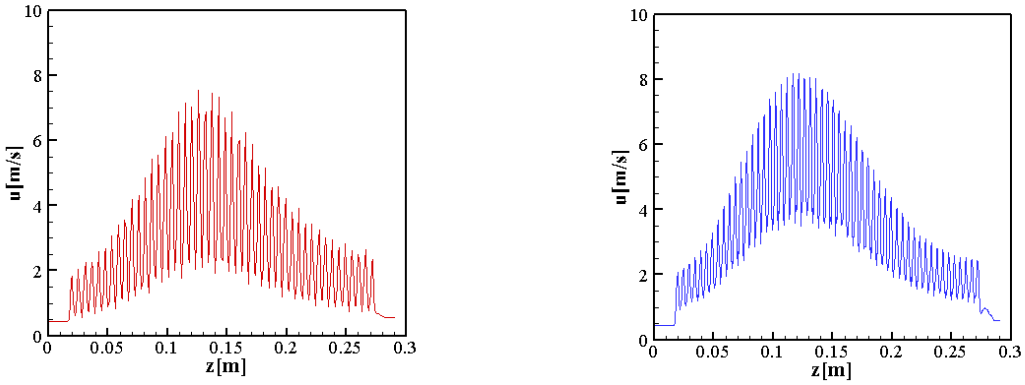

(a) in-line **(b) staggered**

Figure 11. Average velocity of gas

Figure 12 and 13 display the velocity streamlines in the maximum instantaneous velocity region of the packed bed with in-line and staggered at u_0=0.33 and 0.63 m/s for t=250s. It can be seen that the streamline in the packed bed varies greatly with different distribution models. In the in-line model, a symmetrical vortex is generated at the joint of the sphere-sphere, and the flow stagnation occurs here. Since the pores between pellets are narrow and asymmetric, the vortex is relatively small and has different forms in the staggered model. When u_0 increases, the eddy current disturbance at the pores of the two models intensifies. In the packed bed, the air is heated by pellets, which reduces the air density and produces a large local instantaneous velocity. When u_0=0.33 m/s, the maximum instantaneous velocity is 10 m/s for in-line arrangement and 11 m/s for staggered arrangement. When u_0=0.63 m/s, the maximum instantaneous velocity of in-line arrangement is 16 m/s, and that of staggered arrangement is 19 m/s, and the speed gap between them increases.

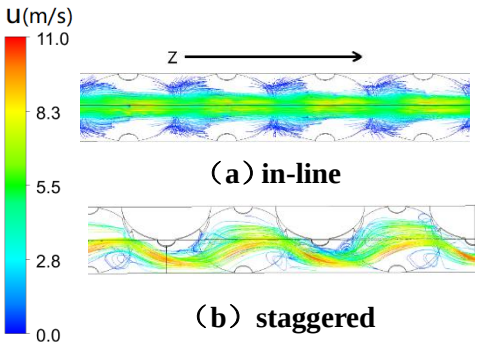

Figure 12. Local streamline in packed bed structures at u_0=0.33 m/s

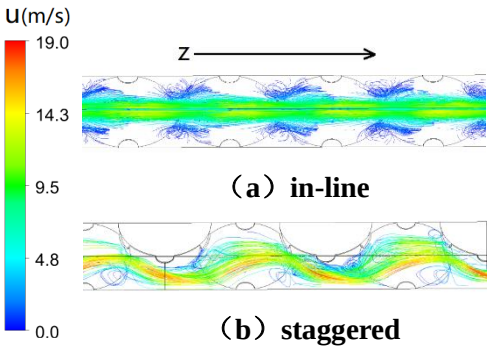

Figure 13. Local streamline in packed bed structures at u_0=0.63 m/s

In the present paper, detailed pore scale models of structured packed beds have been established,

and the influence of pore-scale properties on the pressure drop, macroscopic flow and heat transfer behavior in the packed-bed has been investigated. The main conclusions are as follows:

- The pressure drop increases significantly in the in-line and staggered packed models with high temperature. Compared with staggered model, the pressure drop of in-line distribution is higher. With the increase of inlet velocity, the gap between the two gradually decreases.
- The model of porous media has significant influence on the temperature in the packed bed. The average temperature in the packed bed and the average temperature in the solid and gas phases are different. Compared with the in-line arrangement, the heat wave transfer is slower and the temperature is slightly higher in the staggered model.
- The average velocity in the structured packed bed increases and decreases periodically. Compared with the in-line model, the velocity disturbance in the staggered model is more significant. In in-line model, a large symmetrical vortex occurs in the pore. The vortex is narrow in the staggered model. As the inlet velocity increases, the instantaneous velocity difference in the two models increases.

Although the in-line and staggered sphere packed bed have be examined, the study is inconclusive on the most optimal parameter ratio of packed beds. Therefore, there is much scope for further work on both experiments and theory to achieve generalized principles. Moreover, if more computational power could be available, the simulation of the whole flow field and other forms of packed beds could be attempted. This would be helpful to industrial applications as well as new design of packed beds.

Nomendature

c	specific heat capacity [kJkg^{-1}K^{-1}]	$\overline{T}$	average temperature [K]
d	pellet diameter [mm]	$\overline{u}$	average velocity in z direction [ms^{-1}]
L	total length of packed bed [mm]	u	velocity [ms^{-1}]
P	pressure [Pa]	u_0	gas inlet velocity [ms^{-1}]
q_R	radiant heat flux [Wm^{-2}]	$\overline{\mathbf{v}}$	velocity vector [ms^{-1}]
t	time [s]	x	x coordinate [-]
T	temperature [K]	y	y coordinate [-]
T_0	gas inlet temperature [K]	z	z coordinate [-]
Greek Symbols			
λ	thermal conductivity [Wm^{-1}K^{-1}]	ρ	density [kg m^3]
μ	dynamic viscosity [Pa s]	σ	Stephan-Boltzmann constant [Wm^{-2}K^{-4}]
ε_r	solid surface emissivity [-]		
Subscripts			
g	gas	s	solid
in	inlet of packed bed	out	outlet of packed bed

Acknowledgment

The present work has been supported by the Liaoning province Department of Education fund (LJKMZ20221713 and LJKZ1105).

References

[1] Gautam, A., *et al.,* Experimental investigation of heat transfer and fluid flow behavior of packed bed solar thermal energy storage system having spheres as packing element with pores, *Solar Energy, 204* (2020), pp. 530-541

[2] Kim, G.B., *et al.,* Buoyant convection of a power-law fluid in an enclosure filled with heat-generating porous media, *Numerical Heat Transfer, 45* (2020), 6, pp. 569-582

[3] Eppinger, T., *et al.,* Influence of macroscopic wall structures on the fluid flow and heat transfer in fixed bed reactors with small tube to particle diameter ratio, *Processes, 9* (2021), 4, pp. 689

[4] Toledo, E.C.V., *et al.,* Suiting dynamic models of fixed-bed catalytic reactors for computer -based applications, *Engineering, 3* (2011), pp. 778–785

[5] Prakasam, M.J.S., *et al.,* An experimental study of the mass flow rates effect on flat plate solar water heater performance using Al2O3/water nanofluid, *Thermal Science, 21* (2017), 2, pp. S379-S388

[6] Kondakrindi, K.R., *et al.,* Nanofluids (CuO & TiO2) – Water as heat transfer fluid in a TES system for applications of solar heating-an experimental study, *Thermal Science*, 2023, https://doi.org/10.2298/TSCI221215080K

[7] Cheng, Z.D., *et al.,* Numerical investigations on coupled heat transfer and synthetical performance of a pressurized volumetric receiver with MCRT-FVM method, *Applied Thermal Engineering, 50* (2013), pp. 1044-1054

[8] Villafán-Vidales, H.I., *et al.,* Heat transfer simulation in a thermochemical solar reactor based on a volumetric porous receiver, *Applied Thermal Engineering, 31* (2011), pp. 3377-3386

[9] Calis, H.P.A., *et al.,* CFD Modelling and experimental validation of pressure drop and flow profile in a novel structured catalytic reactor packing, *Chemical Engineering Science*, *56* (2001), 4, pp. 1713-1720

[10] Romkes, S.J.P., *et al.,* CFD Modelling and experimental validation of partical-to-fluid mass and heat transfer in a packed bed at very low channel to particle diameter ratio, *Chemical Engineering Journal*, 96 (2003), 1-3, pp. 3-13

[11] Gunjal, P.R, *et al.,* Computational study of a single-phase flow in packed beds of spheres, *AIChE Journal, 51* (2005), 2, pp. 365-378

[12] Yang, J., *et al.,* Computational study of forced convective heat transfer in structured packed beds with spherical or ellipsoidal particles, *Chemical Engineering Science, 65* (2010), pp. 726–738

[13] Zhu, Q.B., *et al.,* Pore scale numerical simulation of heat transfer and flow in porous volumetric solar receivers, *Applied Thermal Engineering*, *120* (2017), pp. 150-159

[14] Kim, M.H., *et al.,* Computational fluid dynamics assessment of the local hot core temperature in a pebble-bed type very high temperature reactor, *J. Eng. Gas Turbines Power, 131* (2009), pp. 012905-1

[15] Wang, J.Y., *et al.*, Hydraulic and heat transfer characteristics in structured packed beds with methane steam reforming reaction for energy storage, *International Communications in Heat and Mass Transfer, 121* (2021), pp. 105109

[16] Zhdanok, S., *et al.*, Superadiabatic combustion of methaneair mixtures under filtration in a packed bed, *Combustion and Flame, 100* (1995), pp. 221-231

[17] Zhang, J.Y. Numerical Investigation of the Premixed Gases Combustion in Packed bed (in Chinese), Ph. D. thesis, Dalian University of Technology, Dalian, China, 2013

[18] Bedoya, C., *et al.*, Experimental study, 1D volume-averaged calculations and 3D direct pore level simulations of the flame stabilization in porous inert media at elevated pressure, *Combustion and. Flame, 162* (2015), pp. 3740-3754

[19] Bu, S.S., *et al.*, On contact point modifications for forced convective heat transfer analysis in a structured packed bed of spheres, *Nuclear Engineering and Design, 270* (2014), pp. 21-33

Received: 22.04.2023.
Revised: 11.07.2023.
Accepted: 18.08.2023